Mixed-integer linear approximations of AC power flow equations for systems under abnormal operating conditions

Ignacio Aravena
CORE, UC Louvain
ignacio.aravena@uclouvain.be

Deepak Rajan
Lawrence Livermore National Lab.
rajan3@llnl.gov

Georgios Patsakis
IEOR, UC Berkeley
gpatsakis@berkeley.edu

***Abstract*—We present a methodology to generate mixed-integer linear approximations of the AC power flow equations governing lines, transformers (including tap regulators and phase shifters), shunt and series compensators, and consumption responsive to voltage. Our motivation is to employ these models in grid topology optimization of realistic power grids under abnormal or uncommon operating conditions, where usual assumptions for relaxing the power flow equations may not hold. The method constructs piecewise linear approximations of the non-linear power flow equations by minimizing the squared approximation error over a subset of the feasible domain. We test the method using a realistic database for the Chilean system (1548 buses, 1114 lines, 564 transformers). The resulting approximations yield root mean square errors in the order of 0.05pu and are successfully applied to solve a transmission switching instance for the system.**

NOMENCLATURE

Parameters

g_{ij}, b_{ij}	series conductance, susceptance of branch (i,j)
s_{ij}	thermal limit of branch (i,j)
V^L, V^U	upper and lower operational voltage limits
α_c, β_c	exponents of load response to voltage variations of aggregated consumer c

Variables

v_i, θ_i	voltage magnitude and angle of bus i
δ_{ij}	angle difference for branch (i,j) ($\delta_{ij} = \theta_i - \theta_j$)
p_i^{ij}, q_j^{ij}	active and reactive power entering branch (i,j) at bus j
u_{ij}	energization state of branch (i,j) ($u_{ij} \in \{0,1\}$)
w_k, γ_k	voltage and phase shift tap changers at terminal k of power transformers
p_c, s_c, q_c	active power consumption, active load shedding and reactive power consumption of aggregated consumer c

I. INTRODUCTION

The AC power flow equations, which can be expressed as

$$p_i^{ij} = v_i^2 g_{ij} - v_i v_j g_{ij} \cos(\delta_{ij}) - v_i v_j b_{ij} \sin(\delta_{ij}) \quad (1)$$

$$q_i^{ij} = -v_i^2 b_{ij} + v_i v_j b_{ij} \cos(\delta_{ij}) - v_i v_j g_{ij} \sin(\delta_{ij}), \quad (2)$$

for a simple branch, lie at the core of most optimization models for planning and operations in power systems. For high-voltage transmission networks under normal operating conditions, these equations are usually well approximated by the DC power flow equations [1], which ignore voltage and reactive power and focus only on angle differences and active power. The DC power flow equations, however, fall short when modeling systems where the ratio resistance/reactance becomes high, or in conditions where reactive power plays an important role, such as the outcome of topology changes (either short-term transmission switching or transmission expansion planning), during widespread contingencies, or during the restoration sequence following a blackout [2].

Different convex relaxations of the AC power flow equations have been proposed, aiming to extend the application of optimization technology beyond the validity of the DC power flow equations. Jabr [3] introduces a second-order cone relaxation of the AC power flow equations in polar form for distribution networks. Bai *et al.* [4] propose a semidefininite programing relaxation of the power flow equations in rectangular form. Lavaei and Low [5] would later prove the semidefinite relaxation to be exact in many IEEE test cases. Farivar and Low [6], [7] propose a second-order cone relaxation of the branch flow equations, i.e. the power flow equations in terms of currents and voltages (as opposed to power and voltages). Coffrin and Van Hentenryck [8] present a relaxation that uses a polyhedral outer approximation of the sine and cosine terms in the power flow equations, and a first order Taylor approximation around a given operating point to model the dependency with respect to voltage. Coffrin *et al.* [9] extend the previous idea by using a quadratic envelope for the cosine term.

Some of these relaxations have been applied to solve combinatorial problems in power systems. In particular, Bienstock and Muñoz [10] use a sequence of second-order conic and semidefinite relaxations for solving an instance of the transmission switching problem, while Hijazi *el at.* [11] used a quadratic convex relaxation for solving the transmission switching problem over a large set of standard test systems.

In contrast with previous work, our aim is to generate piecewise linear approximations (not necessarily relaxations) of the feasible region defined by the power flow equations for realistic systems. Since our ultimate goal is to embed these approximations into larger combinatorial problems, the models need to be as simple as possible, while still preserving the main characteristics of the power flow equations. We aim for an

approximation that is valid for realistic systems under a wide range of abnormal operating conditions, hence we cannot rely on constructing an approximation around a given operating point, neither can we assume that the system will be in scarcity of reactive power, as done in previous methods for generating piecewise linear approximations [8]. Instead, we generate our approximations by minimizing the squared error in terms of active and reactive power over a representative box of the feasible domain for each branch. Using the approximations, we propose mixed-integer linear programming (MILP) models for transformers with tap regulators and phase shifters, series compensators, and voltage-responsive load at distribution substations. These elements, while abundant in real systems, are usually ignored in the literature.

Our main contributions are: (*i*) a new piece-wise linear approximation of the feasible region defined by AC power flow equations, (*ii*) a new mixed-integer linear programming model for elements of real systems, such as transformers with tap regulators and phase shifters, series compensators and load at distribution substations, and (*iii*) a computational study on a realistic system (based on Chile, with over 1500 buses) that illustrates the tractability and accuracy of our model.

The rest of the paper is organized as follows. Section II introduces the proposed technique to generate piecewise linear approximations of the power flow equations. Section III presents the proposed MILP models for transformers, reactive compensators and consumers. Section IV presents a two-node network example that ilustrates the differences between our approximation and relaxations and approximations present in the literature. Section V describes the Chilean system database used in this study and presentes statistics on the approximation for the Chilean system. Section VI presents the conclusions of the present study along with directions of future research.

II. Piece-wise linear approximation of AC power flow equations

Fitting piece-wise linear approximations to functions is a widely studied problem in optimization. Two main approaches are present in the literature: (*i*) a partition I of the interest domain for the approximation, and a set of slopes $\boldsymbol{a}_i$ and intercepts b_i for each $i \in I$ [12]; and (*ii*) a max- or min-type function with a set of slopes and intercepts (defining implicitly the partition of the interest domain) [13]. In the following, we opt for the first approach and restrict the partition to be boxes for simplicity of the estimation process and of the derived MILP formulations.

A. Approximation of function over a box in n-dimensions

Assume we have a continuous function $f : \mathbb{R}^n \to \mathbb{R}$ that we wish to approximate with a piecewise linear function $\hat{f} : \mathbb{R}^n \to \mathbb{R}$ defined as

$$\hat{f}(\boldsymbol{x}) := \boldsymbol{a}_i^T \boldsymbol{x} + b_i \text{ if } \boldsymbol{x}_i^L \preccurlyeq \boldsymbol{x} \preccurlyeq \boldsymbol{x}_i^U, i \in I,$$

over the box between $\boldsymbol{x}^L$ and $\boldsymbol{x}^U$, respectively, the lower and upper vertex of the interest domain. Let $[\boldsymbol{x}_i^L, \boldsymbol{x}_i^U]$ be the box between $\boldsymbol{x}_i^L$ and $\boldsymbol{x}_i^U$ ($[\boldsymbol{x}^L, \boldsymbol{x}^U] = \cup_{i \in I} [\boldsymbol{x}_i^L, \boldsymbol{x}_i^U]$), $F(i,j)$ be the facet between the adjacent cells i, j and $\mathcal{F}$ the set of adjacents pairs of cells. Then, the $\boldsymbol{a}_i, b_i$ for all $i \in I$ that minimizes the error can be determined using (3)–(4). The objective function (3) corresponds to the squared total error of the approximation over the interest domain, while constraints (4) enforce continuity of the approximation.

$$\min_{\boldsymbol{a}, b} \quad \sum_{i \in I} \int_{[\boldsymbol{x}_i^L, \boldsymbol{x}_i^U]} (\boldsymbol{a}_i^T \boldsymbol{x} + b_i - f(\boldsymbol{x}))^2 d\boldsymbol{x} \tag{3}$$

$$\text{s.t.} \quad \boldsymbol{a}_i^T \boldsymbol{x} + b_i = \boldsymbol{a}_j^T \boldsymbol{x} + b_j \quad \forall x \in F(i,j), \forall (i,j) \in \mathcal{F} \tag{4}$$

In practice, we approximate the integrals in the objective (3) using the Gauss-Legendre quadrature along each dimension, leading to a convex quadratic problem on $\boldsymbol{a}, b$. The literature [12] suggests to reformulate the continuity constraints (4) by enforcing continuity on all the vertices of each facet, leading to an exponential number of constraints per facet. Instead, we reformulate constraints (4) for each facet $F(i,j)$ by enforcing continuity on a set of n affine independent points within $F(i,j)$, which is a sufficient condition to ensure continuity of the approximation. This reformulation of the continuity constraints leads to a linear number of constraints per facet, significantly reducing the problem size in higher dimensions.

B. Approximation of power flow equations of system branch

To generate approximations for the power flow equations, i.e. to approximate $p_i^{ij}(v_i, v_j, \delta_{ij})$ and $q_i^{ij}(v_i, v_j, \delta_{ij})$ as defined in (1)–(2), using the procedure described in the previous section, we first need to define the interest domain of the approximation and the partition.

A naive selection of the domain can lead to infeasibility of the approximation, as explained by the example of Fig. 1. To prevent these problems we define the interest domain by averaging inner- and outer-box approximations of the set of feasible tuples (v_i, v_j, δ_{ij}), Ω^{ij}, defined according to:

$$\Omega^{ij} = \{(v_i, v_j, \delta_{ij}) \mid V^L \leq v_k \leq V^U,\ p_k^{ij}(v_i, v_j, \delta_{ij})^2 + q_k^{ij}(v_i, v_j, \delta_{ij})^2 \leq s_{ij}^2, k = i, j\}.$$

We obtain an inner box by maximizing the volume of an hyper-rectangle containing $(v_i, v_j, \delta_{ij}) = (1, 1, 0)$ and with all its vertices within Ω^{ij}. To obtain an outer box we maximize/minimize each coordinate of (v_i, v_j, δ_{ij}) while remaining within Ω^{ij}. The lower and upper vertices of the inner and outer box are then averaged coordinate-wise to obtain the lower and upper vertices of the interest domain $\boldsymbol{x}^L$ and $\boldsymbol{x}^U$, which will be different for every branch. As Ω^{ij} is a non-convex region, there might be points inside the interest domain which lie outside Ω^{ij}. For those points, if they appear as knots of the Gauss-Legendre quadrature during the approximation of the integrals of (3), we assign them a weight of zero in order to prevent them from biasing the approximation. Following [8], we partition the interest domain only across the δ_{ij} coordinate, whenever it is necessary depending on the resistance/reactance ratio, as explained in Fig. 2. The partition is done by dividing the range for δ_{ij} in intervals of equal cumulated curvature of q_i^{ij} or p_i^{ij}, depending on the resistance/reactance ratio, for

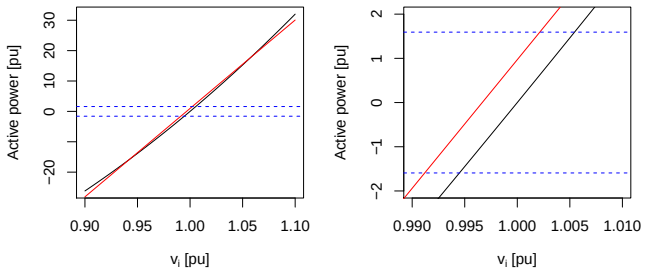

Fig. 1. Approximation of the active power in line "P.Azucar 110kV" (part of the Chilean system) between feasible limits [0.9,1.1] for voltage, shown at $v_j = 1$ and $\delta_{ij} = 0$. The true active power is shown in black while the approximation is shown in red. Horizontal blue lines correspond to the thermal limits of the line. While the approximation behaves well across the range [0.9,1.1], when restricted to the feasible domain it presents a significant bias that can render the approximation of the power flow equations infeasible.

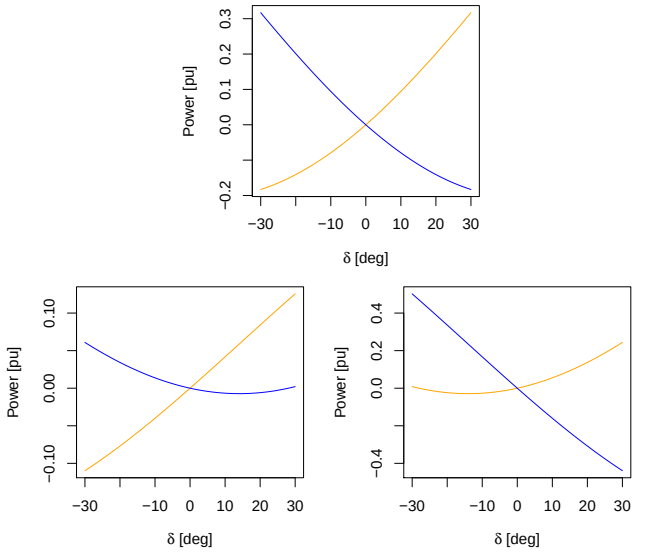

Fig. 2. Effect of resistance/reactance ratio in the power entering a branch, with $v_i = v_j = 1$. The top figure corresponds to a ratio of 1, while the bottom figures correspond to ratios of 1/4 and 4 (from left to right). Active power is presented in orange and reactive power in blue. For resistance/reactance smaller than 2/3 we model the reactive power using a piecewise function and active power as an affine function, while the converse is true for ratios greater than 3/2. For 2/3 $\leq$ resistance/reactance $\leq$ 3/2 both active and reactive power are approximated by affine functions.

$v_i = v_j = 1$. This results in an partition with smaller boxes in zones with higher curvature, such as the valleys caused by cosine terms in Fig. 2.

III. MILP Models of Power System Elements

We adapt the multiple choice model, referred to as *M2* in [14], to approximate the power flow equations (1)–(2) for a branch while accounting for topology changes, i.e. that the branch can be de-energized. Using additional variables $u_{ij}^q \in \{0,1\}$ and δ_{ij}^q, for $q \in \{1,\ldots,Q\}$, the equations of the multiple choice model to select the range of δ_{ij} can be written as (5)–(7), where Δ_{ij} is an absolute bound on δ_{ij}. Then the power flow equations are approximated as (8) for q_i^{ij}, with analogous expression for p_i^{ij}, if required. Here $M_{ij,q}^L, M_{ij,q}^U$ are bounds that consider that δ_{ij}^q becomes zero when the branch is de-energized.

$$u_{ij} = \sum_{q=1}^{Q} u_{ij,q} \tag{5}$$

$$-\Delta_{ij} \cdot (1 - u_{ij}) \leq -\delta_{ij} + \sum_{q=1}^{Q} \delta_{ij}^q \leq \Delta_{ij} \cdot (1 - u_{ij}) \tag{6}$$

$$\delta_q^L \cdot (1 - u_{ij,q}) \leq \delta_{ij}^q \leq \delta_q^U \cdot (1 - u_{ij,q}) \tag{7}$$

$$\begin{aligned} M_{ij,q}^L(1 - u_{ij,q}) \leq -q_i^{ij} + a_{q,1} v_i + a_{q,2} v_j + \\ a^{q,3}\delta_{ij}^q + b_q \leq M_{ij,q}^U(1 - u_{ij,q}) \end{aligned} \tag{8}$$

While equations (5)–(8) are sufficient to describe a generic branch and its de-energization as an open circuit, real power systems contain a range of other elements which are usually simplified in common test cases, such as those used in [8], [9]. Next, we detail the elements we have found while working with the realistic instance described in subsection V-A.

A. Shunt and series reactive compensators

Depending on the application, reactive compensators might be installed as shunts in substations or in series with transmission lines, to regulate reactive power. We consider 3 main categories of reactive compensators:

- Shunt controllable reactive compensators: equipment with power electronics that can control the reactive power, irrespective of the voltage level. They can be modeled as an injection of reactive power between certain bounds.
- Shunt sectioned reactive compensators: equipment such as shunt capacitors or reactors, with multiple stages. Their reactive injection depends linearly on the number of stages connected and quadratically on the voltage. By relaxing the discrete staging they can be modeled as a variable injection of reactive power to the system, bounded by a linear approximation of the squared voltage over its operational limits.
- Series compensators: large reactors or capacitors connected in series with transmission lines for operating under different load regimes. Unlike transmission lines, however, when de-energized these elements are not opened but short-circuited. Hence, in addition to constraints (5)–(7), we also enforce constraints (9)–(12).

$$(V^L - V^U) \cdot u_{ij} \leq v_i - v_j \leq (V^L - V^U) \cdot u_{ij} \tag{9}$$

$$-\Delta_{ij} u_{ij} \leq \delta_{ij} \leq \Delta_{ij} u_{ij} \tag{10}$$

$$-2s_{ij} u_{ij} \leq p_i + p_j \leq 2s_{ij} u_{ij} \tag{11}$$

$$-2s_{ij} u_{ij} \leq q_i + q_j \leq 2s_{ij} u_{ij} \tag{12}$$

B. Transformers, voltage tap changers and phase-shifters

The main intricacies that arise when modeling transformers of an actual system are: (*i*) The nominal transformation ratios of a transformer might not match exactly the base per unit values of the system, e.g. there might be a 500kV/230kV transformer connected between nominal levels 500kV/220kV,

which is resolved by introducing scale factors for the voltage. (*ii*) Voltage tap changers introduce additional modifications to the voltage bounds that enter the power flow equations (modifying Ω^{ij}). (*iii*) Transformers can possess more than two windings. A 2-winding transformer can be directly modeled as a branch. We model an m-winding transformer with a star model with m piece-wise linear functions (one per winding) and two additional variables to represent the magnitude and angle of the voltage at the node at the center of the star, v_0, θ_0, respectively. We model each winding k as a branch, using

$$\begin{aligned}\delta_{k0} &:= \theta_{i(k)} + \gamma_k - \theta_0,\\ M^L_{kq}(1-u_{k0,q}) &\leq -q_{i0} + a_{q,1}(v_{i(k)} + w_k) +\\ a_{q,2}v_0 + a_{q,3}\delta^q_{k0} + b_q &\leq M^U_q(1-u_{k0,q}),\end{aligned}$$

while also enforcing power balance at the center node of the star.

C. Voltage-responsive demand at distribution substations

Passive loads typically change their consumption with voltage variations, following a monomial load model:

$$\begin{aligned}p_c + s^P_c &= P_c \cdot v^{\alpha_c}_{i(c)}\\ q_c &= Q_c \cdot v^{\beta_c}_{i(c)} \cdot p_c/(P_c \cdot v^{\alpha_c}_{i(c)}),\end{aligned}$$

where it is enforced that the same proportion of active and reactive power are shed at the same time (implicitly assuming that the load is homogenous). To retain this behaviour, we construct linear approximations of the voltage terms $v^{\alpha_c}_{i(c)}, v^{\beta_c-\alpha_c}_{i(c)}$, which lead to constraints (13)–(14) for the load model.

$$p_c + s^P_c = a^P_c v_{i(c)} + b^P_c \tag{13}$$

$$1/a^Q_c q_c - b^Q_c/a^Q_c p_c = p_c v_{i(c)} \tag{14}$$

Finally, the $p_c v_{i(c)}$ product in the reactive consumption constraint is approximated by its McCormick envelopes [15].

IV. Illustrative example: Energizing a long line

In order to illustrate the differences between the approximation of the power flow equations proposed in this paper and relaxations and approximations proposed in the literature we employ the two-node network Fig. 3. For this network, we would like to determine whether the line between buses 1 and 2 can be energized, while keeping the voltage at bus 1 fixed in 1 p.u. and the voltage at bus 2 between 0.9 p.u. and 1.1 p.u. This problem is important when designing restoration sequences for power systems [16].

We use the QC relaxation [9], as an example of non-linear relaxations, and the LP approximation [8]. Our selection of the QC relaxation is based on (*i*) that it is stronger than SOCP relaxations and (*ii*) that SDP relaxations are computationally too expensive to be included within combinatorial problems.

From circuit analysis, we obtain that in order to energize the line, the generator at bus 1 will need to inject -119.9MVAr to the network. As the generator can inject -80.7MVAr at best, the line cannot be energized. The required (infeasible) operation point for the line is indicated by a black circle in Fig. 4. The QC relaxation finds that the line can be energized, due

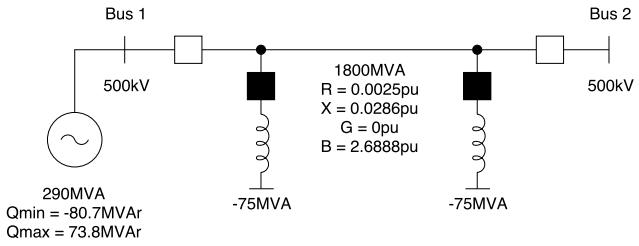

Fig. 3. Single line diagram of the two-node network for long line energization. This ficticial network is composed by elements of the Chilean system [17]; the generator correspond to unit 1 of the Pehuence power plant, and the line – with its shunt reactors – correspond to circuit 2 of line "Ancoa - Alto Jahuel 500kV". Values in p.u. use base 100MVA.

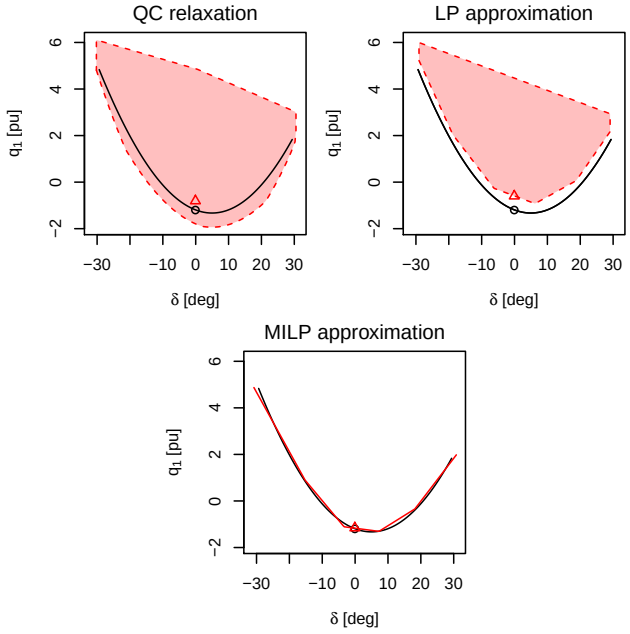

Fig. 4. Feasible domains for q^{12}_1 as a function of δ, considering (1), (2) and enforcing $v_2 = v^{AC}_2$, for: (*i*) the QC relaxation [9], (*ii*) LP approximation (cold-start LPAC, 5 intervals) [8] and (*ii*) our MILP approximation (5 intervals). For (*i*) and (*ii*) the red-shaded area, limited by dashed lines, indicates the range of possible values for q^{12}_1 at each δ. For (*iii*), the continuous red line indicates the value of the approximation at each δ. In all cases, the red triangle indicates the solution (or infeasible point) obtained when considering power balance at both buses, the black line indicates the true value of q^{12}_1 at each δ, and the black circle indicates the AC infeasible point.

to the convex envelope used to model the cosine term in (1)–(2). The LP approximation overestimates the reactive power consumed by the line because of assuming a unitary voltage, leading also to the conclusion that the line can be energized. Even without this overestimation, the LP approximation can demand the injection of physically meaningless reactive power because of the piece-wise linear envelope used to model the cosine term. Finally, the MILP approximation constructed with the procedure outlined in section II correctly identifies that the energization of the line is not feasible. Cases where the system is at excess of reactive power can appear locally in a system due to congestion, line switching or during power system restoration. As demonstrated by the example,

TABLE I
AVERAGE ERROR IN THE APPROXIMATION OF POWER FLOW EQUATIONS FOR BRANCHES FOR DIFFERENT VALUES OF Q. RESULTS EXPRESSED IN PU OF 100MVA BASE.

Q	Lines		Transformers	
	RMSE p [pu]	RMSE q [pu]	RMSE p [pu]	RMSE q [pu]
1	0.066	0.096	0.024	0.022
2	0.066	0.041	0.024	0.013
4	0.065	0.037	0.024	0.011

relaxations and approximations proposed in the literature may lead to inaccurate evaluation of decisions in such scenarios.

V. NUMERICAL EXPERIMENTS

We implement the piecewise linear approximation method in Julia [18], using JuMP [19] to formulate the mathematical programs and Ipopt [20] as non-linear solver. We checked the feasibility of the approximated power flow equations using Gurobi to solve the resulting MILP problems.

A. A realistic test system: the Chilean network

We constructed a realistic database for the Chilean Central Interconnected System ("Sistema Interconectado Central", SIC) using the information publicly available in the website of the system operator [17]. The system consists of 1548 buses with nominal voltages ranging between 0.3kV and 500.0kV, 1114 lines, 433 2-winding transformers, 131 3-winding transformers, 159 shunt compensators, 14 series compensators, 297 generators and 605 loads. 509 out of the 564 transformers have voltage tap changers, and there are 7 phase shifters.

The system contains very short lines, connecting neighboring substations. These lines were modeled as short circuits in order to avoid numerical ill-conditioning. Among the lines, we found 84 cases for which the ratio resistance/reactance was greater than 1. For loads, the values of α_c oscillate around 1, while the values of β_c oscillate around 3, showing that reactive power demand is very dependent on voltage variations.

B. Approximation results

We applied the method to generate approximations to the Chilean network. The accuracy of the approximation for branches of the network is presented in Table I. Using the approximation with $Q = 1$ we were able to solve an AC approximation of the transmission switching problem for the Chilean network using Gurobi in 149 seconds.

VI. CONCLUSIONS

We presented a method for generating piecewise linear approximations of the power flow equations based on least squares fitting instead of approximations around an operating point. We applied the method to a realistic database for the Chilean grid, obtaining an average error in the order of 0.05pu.

Future extensions of the present work will include a detailed test of the approximation in transmission switching instances under contingencies and the application of the approximation to the restoration and black-start allocation problem, which is critical for systems in seismic zones such as the Chilean, Japanese and California systems.

ACKNOWLEDGMENT

Some of this work was performed under the auspices of the U.S. Department of Energy by Lawrence Livermore National Laboratory under contract DE-AC52-07NA27344. The authors would like to thank Gurobi Optimization for providing licenses to the Gurobi mathematical programming solver.

REFERENCES

[1] B. Stott, J. Jardim, and O. Alsac, "DC power flow revisited," *IEEE Transactions on Power Systems*, vol. 24, no. 3, pp. 1290–1300, 2009.

[2] C. Coffrin and P. V. Hentenryck, "Transmission system restoration: Co-optimization of repairs, load pickups, and generation dispatch," in *2014 Power Systems Computation Conference*, pp. 1–8, 2014.

[3] R. A. Jabr, "Radial distribution load flow using conic programming," *IEEE Transactions on Power Systems*, vol. 21, no. 3, pp. 1458–1459, 2006.

[4] X. Bai, H. Wei, K. Fujisawa, and Y. Wang, "Semidefinite programming for optimal power flow problems," *International Journal of Electrical Power & Energy Systems*, vol. 30, no. 6, pp. 383 – 392, 2008.

[5] J. Lavaei and S. H. Low, "Zero duality gap in optimal power flow problem," *IEEE Transactions on Power Systems*, vol. 27, no. 1, pp. 92–107, 2012.

[6] M. Farivar and S. H. Low, "Branch flow model: Relaxations and convexification – part i," *IEEE Transactions on Power Systems*, vol. 28, no. 3, pp. 2554–2564, 2013.

[7] M. Farivar and S. H. Low, "Branch flow model: Relaxations and convexification – part ii," *IEEE Transactions on Power Systems*, vol. 28, no. 3, pp. 2565–2572, 2013.

[8] C. Coffrin and P. V. Hentenryck, "A linear-programming approximation of AC power flows," *INFORMS Journal on Computing*, vol. 26, no. 4, pp. 718–734, 2014.

[9] C. Coffrin, H. L. Hijazi, and P. V. Hentenryck, "The QC relaxation: A theoretical and computational study on optimal power flow," *IEEE Transactions on Power Systems*, vol. 31, no. 4, pp. 3008–3018, 2016.

[10] D. Bienstock and G. Muoz, "Approximate method for AC transmission switching based on a simple relaxation for ACOPF problems," in *2015 IEEE Power Energy Society General Meeting*, pp. 1–5, 2015.

[11] H. Hijazi, C. Coffrin, and P. V. Hentenryck, "Convex quadratic relaxations for mixed-integer nonlinear programs in power systems," *Mathematical Programming Computation*, vol. 9, no. 3, pp. 321–367, 2017.

[12] A. Toriello and J. P. Vielma, "Fitting piecewise linear continuous functions," *European Journal of Operational Research*, vol. 219, no. 1, pp. 86 – 95, 2012.

[13] A. Magnani and S. P. Boyd, "Convex piecewise-linear fitting," *Optimization and Engineering*, vol. 10, no. 1, pp. 1–17, 2009.

[14] S. Sridhar, J. Linderoth, and J. Luedtke, "Locally ideal formulations for piecewise linear functions with indicator variables," *Operations Research Letters*, vol. 41, no. 6, pp. 627 – 632, 2013.

[15] G. P. McCormick, "Computability of global solutions to factorable nonconvex programs: Part i — convex underestimating problems," *Mathematical Programming*, vol. 10, no. 1, pp. 147–175, 1976.

[16] G. Patsakis, D. Rajan, J. Rios, and S. Oren, "Optimal black start allocation for power system restoration," Tech. Rep. http://www.optimization-online.org/DB_HTML/2018/02/6450.html, Optimization Online, 2018.

[17] CEN Chile, "Infotecnica." http://infotecnica-sic.coordinadorelectrico.cl/ (in Spanish). Accessed: 2017-09-30.

[18] J. Bezanson, A. Edelman, S. Karpinski, and V. B. Shah, "Julia: A fresh approach to numerical computing," *SIAM Review*, vol. 59, no. 1, pp. 65–98, 2017.

[19] I. Dunning, J. Huchette, and M. Lubin, "JuMP: A modeling language for mathematical optimization," *SIAM Review*, vol. 59, no. 2, pp. 295–320, 2017.

[20] A. Wächter and L. T. Biegler, "On the implementation of an interior-point filter line-search algorithm for large-scale nonlinear programming," *Mathematical Programming*, vol. 106, no. 1, pp. 25–57, 2006.

[21] I. A. Hiskens and R. J. Davy, "Exploring the power flow solution space boundary," *IEEE Transactions on Power Systems*, vol. 16, no. 3, pp. 389–395, 2001.